LASER INTERFEROMETER GRAVITATIONAL WAVE OBSERVATORY
- LIGO -
CALIFORNIA INSTITUTE OF TECHNOLOGY
MASSACHUSETTS INSTITUTE OF TECHNOLOGY

Technical Note **LIGO-T2100160–v1** 2021/09/28

Optimal State-Space Estimation of Interferometer Mode-Matching

Mark Nguyen

California Institute of Technology
LIGO Project, MS 18-34
Pasadena, CA 91125
Phone (626) 395-2129
Fax (626) 304-9834
E-mail: info@ligo.caltech.edu

Massachusetts Institute of Technology
LIGO Project, Room NW22-295
Cambridge, MA 02139
Phone (617) 253-4824
Fax (617) 253-7014
E-mail: info@ligo.mit.edu

LIGO Hanford Observatory
Route 10, Mile Marker 2
Richland, WA 99352
Phone (509) 372-8106
Fax (509) 372-8137
E-mail: info@ligo.caltech.edu

LIGO Livingston Observatory
19100 LIGO Lane
Livingston, LA 70754
Phone (225) 686-3100
Fax (225) 686-7189
E-mail: info@ligo.caltech.edu

http://www.ligo.caltech.edu/

1 Abstract

LIGO's current detectors rely on a system of adaptive optics to carry out highly sensitive measurements, but they lack an optimal control system. In response, we have adopted the Kalman filter formalism to systematically derive a more optimal estimate of the state of the resonant spatial mode of each of the optical cavities by allowing this formalism to statistically weigh both measurement data and predicted state parameters. The filter is capable of accessing the plethora of information that is considered inaccessible by the current suboptimal control system, and then using that information to narrow down the location of the actual state in relation to the desired state. Python simulations are being run on a simple one arm cavity housing two mirrors being lazed by an input beam of an arbitrary mode. Our goal is to eventually be able to integrate this new control system within LIGO's current and future adaptive optics systems to calculate real time estimates of the state of the interferometer.

2 Introduction

In 1916, Albert Einstein theorized "ripples in space-time" known as gravitational waves in his paper on general relativity. It is well understood from this publication that Einstein's definition of gravity differed from Issac Newton's in that Einstein said that gravity is space-time curvature as opposed to Newton stating that gravity is an attractive force or rather an interaction between two objects in only space. Further deviating from the Newtonian gravity explanation, Einstein proposed that gravity was actually the result of a wave of spacetime curvature propagating at the speed of light through not only the three dimensions of space as we know it, but through time as well. These waves would only be caused by the motion of massive astrophysical objects like colliding black holes, supernovae, and colliding neutron stars.

Although it might have been outlandish when it was first proposed and even shook the foundation of modern physics at the time, general relativity mathematics has proven to be correct with its role in increasing the precision of global positioning systems. It was not until an effort designed to detect these waves by the Laser Interferometer Gravitational-Wave Observatory (LIGO), which set out to find evidence of their existence, that Einstein's theoretical predictions would be visually observed and recorded. The first gravitational wave event to be detected and measured was in the year 2015 as a result of the observation of two LIGO detectors during a merger of a pair of black holes into a single black hole. Since that historic event, LIGO has detected 49 more accounts of gravitational waves, some because of the collision of black holes like the first detection and others as a result of supernovae and colliding neutron stars. This effort to detect gravitational waves is no where near ending as work is being done on the current detectors to increase the rate and efficiency of detection by reducing surrounding unwanted noise.

LIGO has achieved a large feat by managing to detect gravitational waves at the sites of extreme astrophysical phenomena of the universe; however, astrophysics is not the only benefiter of these discoveries. Optical physics has been further advanced as a result. Although these extraordinary optical instruments have assisted with the numerous detections, they

still have limitations that can further be improved. There are current systems in place to reduce these noise limitations and one of them is known as the thermal compensation system (TCS). As seen by the layout of Advanced LIGO in Figure 2 there are two actuators that "serve to correct dynamic changes in the ITM and ETM surface curvatures and substrate lenses and are also used to remove static lenses in the ITM substrates[...]" The limitation that exists with this system is that "one cannot actuate with the TCS actuators to affect the SRC mode without also affecting the PRC mode." Furthermore, the true spatial modes of the different interferometer cavities are the hidden state of the system. The hidden state is the result of having measurements and diagnostic signals that are sensitive to the cavity modes but are not directly measured by the system. In an effort to mitigate this issue and gain information about the hidden states, the Kalman filter will be implemented to infer the hidden state.

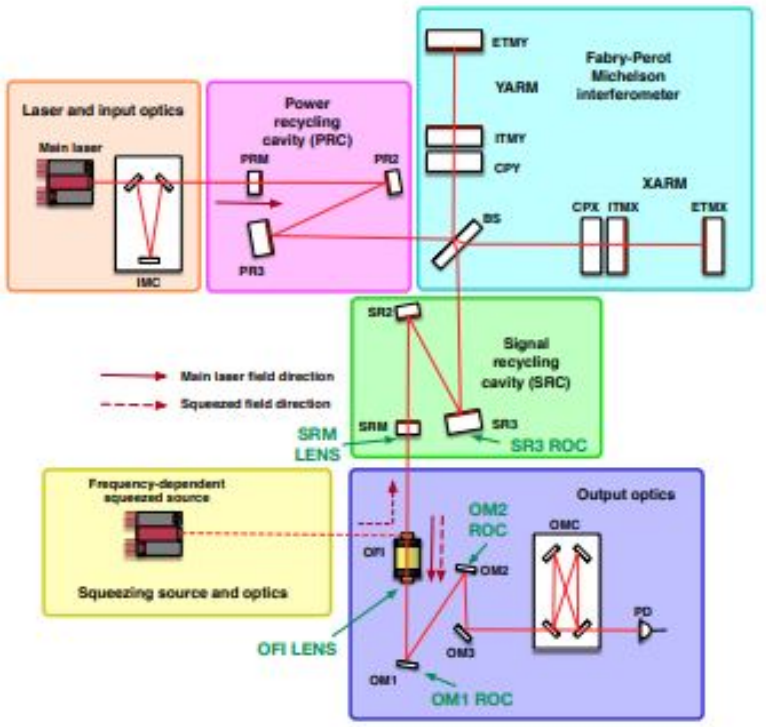

Figure 1: Thermal compensation system with a pair of actuators [2]

3 Kalman Filter

Kalman filters are not a new invention and in fact have been "the most widely used prediction algorithm". The filter essentially takes in information about a current state and then predicts the next state based on this initial state. The Kalman filter's role in "relatively simple state space estimation" has been applied to other physical systems. For example, in radar systems as shown in Figure 1, the use of Kalman filters can increase the accuracy in which an aircraft's position and velocity can be monitored. In order to use a Kalman filter, the function must

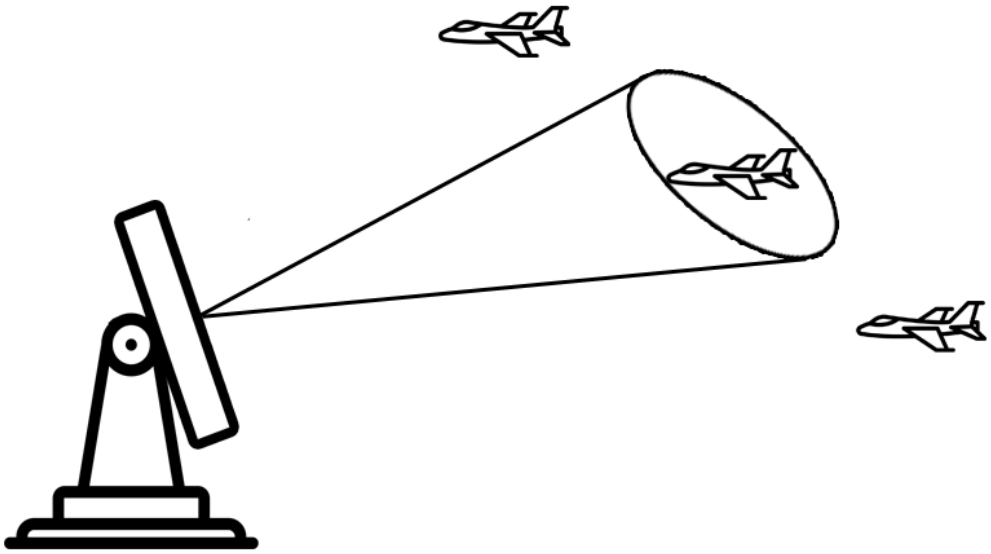

Figure 2: Kalman Filter used as a prediction algorithm in radar systems [4]

$$\begin{cases} x = x_0 + v_{x0}\Delta t + \frac{1}{2}a_x\Delta t^2 \\ y = y_0 + v_{y0}\Delta t + \frac{1}{2}a_y\Delta t^2 \\ z = z_0 + v_{z0}\Delta t + \frac{1}{2}a_z\Delta t^2 \end{cases}$$

Figure 3: Newtons Equations of Motions in three dimensions [4]

either be linear or differentiable. Relatively simple mathematical differentiable functions that may be used in such a radar system are shown in Figure 3 where "the target parameters $[x,\ y,\ z,\ v_x,\ v_y,\ v_z,\ a_x,\ a_y,\ a_z]$ are called a System State." Having the system of equations from Figure 3 which is also known as the "Dynamic Model" along with the current system state, an estimation about a future state can be predicted within a relative margin of error. It is well known that in the real world, these Newtonian equations of motion are not the only thing dictating an object's behavior as there are external factors that contribute to the system state that affect its motion. To make an accurate prediction of a future state, it is necessary that these external factors, or what is referred to as noise in our case, be taken into account. The plan is to implement this same technology in gravitational wave detection systems to solve the aforementioned mystery of the hidden state.

The Kalman filter's implementation is meant to be able to "optimally estimate the current state of the [LIGO] interferometer". Specifically, an extended Kalman filter with "extended" referring "to the fact that the Kalman filter contains non-linear state propagation functions", will be implemented for the sole purpose of mode-matching an input laser beam. The electric field of an optical beam is represented as follows where u_{nm} describes the "spatial properties of the beam", "a_{jnm} as complex amplitude factors, and ω_j is... the angular frequency and $k_j = \omega_j/c$". The intensity of this beam is unlike a plane wave and would actually resemble an intensity distribution. The goal is to have the curvature of the beam's wavefront match the curvature of the optical cavity. Figure 4

$$E(t,x,y,z) = \Sigma_j \Sigma_{n,m} a_{jnm} u_{nm}(x,y,z) exp(i(\omega_j t - k_j z)) \tag{1}$$

Utilizing this equation of the electric field of a Gaussian laser beam, one can proceed

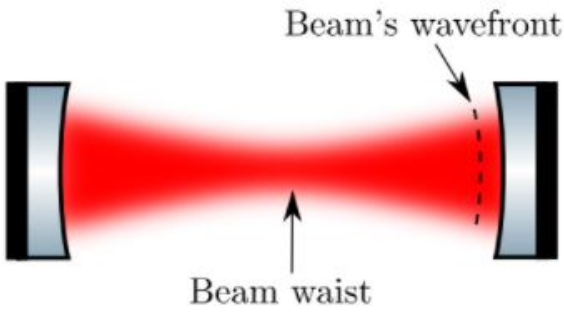

Figure 4: Laser beam front mode-matched with optical cavity [2]

with calculating the mode matching overlap function. For the purpose of demonstrating this method of calculation, one can observe the simple one arm two mirror cavity of the Michelson interferometer setup on LIGO's system. The radii of curvature of the ITM and ETM are 1935 and 2024 meters respectively, the length of the arm is four kilometers, and the wavelength of the optical cavity is 1064 nanometers. The size of the beam waist and its position on the optical axis are necessary parameters to obtain a solution to the mode matching overlap function and is calculated with the following system of equations relating

them:

$$\begin{cases} R_I = -z_0 + \frac{z_R^2}{-z_0} \\ R_E = L - z_0 + \frac{z_R^2}{L - z_0} \end{cases} \tag{2}$$

where $z_R = \frac{\pi \times w_0^2}{\lambda}$ is defined as the Rayleigh range, R_I and R_E is the input and exit test mass respectively, L is the length of the interferometer arm, and z_0 the beam waist position. For mathematical convenience, we solve for z_0, the beam waist position, using this system of equations. Using algebraic manipulation to isolate z_R we get two equations that both contain z_0:

$$\begin{cases} -z_0 R_I + z_0^2 = -z_R^2 \\ R_E(L - z_0) - (L - z_0)^2 = z_R^2 \end{cases} \tag{3}$$

Using the elimination method, we are able to come up with the following relation and numerical value in units of meters:

$$z_0 = \frac{-R_E L + L^2}{-R_I - R_E + 2L} \tag{4}$$

$$z_0 = 1840.5m \tag{5}$$

After obtaining that result, the numerical value can be substituted in the same equation above that was previously used to solve for z_0. Doing so, gives the beam waist size

$$w_0 \approx 0.01 \tag{6}$$

The mode matching function is set up as the following integral:

$$\int_0^{2\pi} \int_0^{\infty} EU = \int_0^{2\pi} \int_0^{\infty} \sqrt{\frac{2}{\pi}} \frac{1}{w_0} e^{-\frac{r}{\alpha w_0}} e^{-\frac{r}{w_0}} r dr d\theta \tag{7}$$

Assuming that the mode of the incoming laser beam is the same as the mode of the optical cavity, we are allowed to make $\alpha = 1$. Evaluating this normalized integral we get that the amplitude of the incoming wave should equal 1.

Similar to having the dynamic model along with the current state in the general use of a Kalman filter, "knowledge of the input beam and TEM00 mode combined with our model engine (state-propagation function) allows [...] an a priori estimate of the mode-matching." The mode matching itself will be measured simultaneously with some uncertainty. The ideal estimate will be a combination of this direct mode matching measurement with the prediction and the optimal weight of the combination determined by the Kalman filter.

The next logical step after doing these calculations analytically on paper was to code them into Python to see if the same results could be obtained. Since the mathematics shown above is more convenient for the one arm cavity than it is for a more complex system, the next rational step was to check that these values were consistent with the matrix operations associated with the ABCD matrix. This matrix method allows for the same results obtained above to be neatly packed into one q parameter, which is simply just a complex number that holds a great deal of information about the system. Elements of the ABCD matrix are

```
#Cavity ABCD Matrix
cav_matrix(RoC_i, RoC_e, L = l, n1 = 1)
```

```
array([[ 3.92543374e+00, -6.28571429e+03],
       [ 1.76495017e-03, -2.57142857e+00]])
```

Figure 5: Code representation of the cavity ABCD Matrix

```
#Gets the q parameter of the one arm cavity
M = cav_matrix( RoC_i, RoC_e, L = l, n1 = 1.)
get_cav_q(M)
```

```
(1840.5228758169933+416.99797157807234j)
```

Figure 6: q parameter of the one arm cavity

substituted into this quadratic equation and the q parameter associated with the cavity is determined through some simple algebra.

This complex number holds a lot of information about the system, most notably the beam waist position and the beam size. It is convenient to output these values into Python to use in later functions.

```
#Unpacks the q parameter for the cavity
q =get_cav_q(M)
unpack_q(q, wl)
```

```
{'w0': 0.011884005629066684,
 'z': 1840.5228758169933,
 'zR': 416.99797157807234,
 'RoC': 1935.0000000000002,
 'w_in': 22.427142542212 23}
```

Figure 7: Unpacking q

The variables "w0" and "z" are shown to be consistent to the beam waist size and position respectively.

$$Cq_{cav}^2 + (D - A)q_{cav} - B = 0 \tag{8}$$

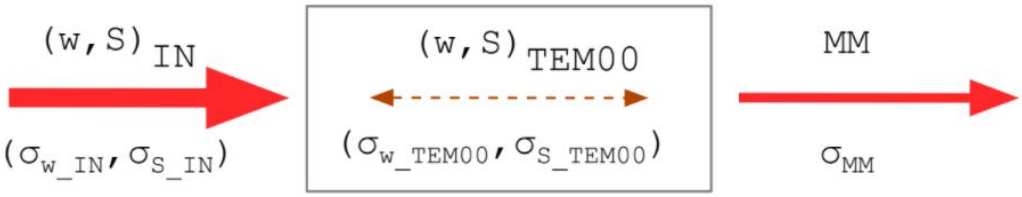

Figure 8: Input laser beam injected into a "TEM00 eigenmode" and the output mode-match is measured [2]

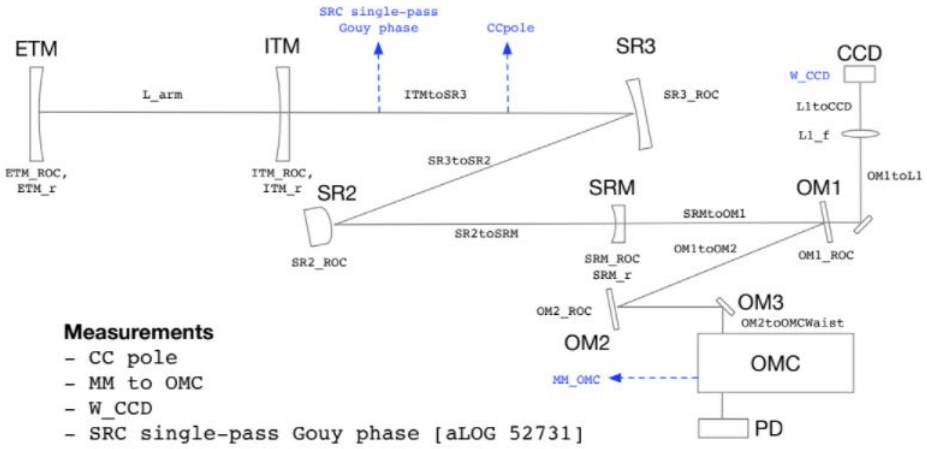

Figure 9: More complex Kalman filter application [2]

4 Objective

The purpose of the project becomes apparent when examining the ability of the Kalman filter to fulfill the outstanding requirement of LIGO detectors. Following the relatively simple description of mode-matching with one laser beam in Figure **??**, one can see that the plan is to eventually scale the potential of the Kalman filter up to a more complicated system like the one in Figure **??**. Similar, yet more intricate compared to the structure of combining the measurements of the mode-matching and the prediction that is to be weighted by the Kalman filter, this more complex system will essentially take in multiple uncertain measurements.

5 Approach

The Kalman filter was implemented in Python. The first couple of weeks was spent learning the prerequisite knowledge of Gaussian laser beams, which included the beam waist, also known as the minimum distance of the beam away from the optical axis, and the beam waist's position on the optical axis. The last few weeks of the program were spent finalizing the plots demonstrating the effectiveness of the Kalman filter.

6 Results

The Python simulations produced three distinct behaviors that when placed on the same coordinate plane displays how the a posterior estimate is preferred over the a priori estimate as the model for estimating the true state of the sample interferometer.

This first plot was generated with static parameters that resembled the actual measurements that describe the LIGO interferometer. For this ideal simulated environment, the plot shows the true state, which is unknown to the real life measurements.

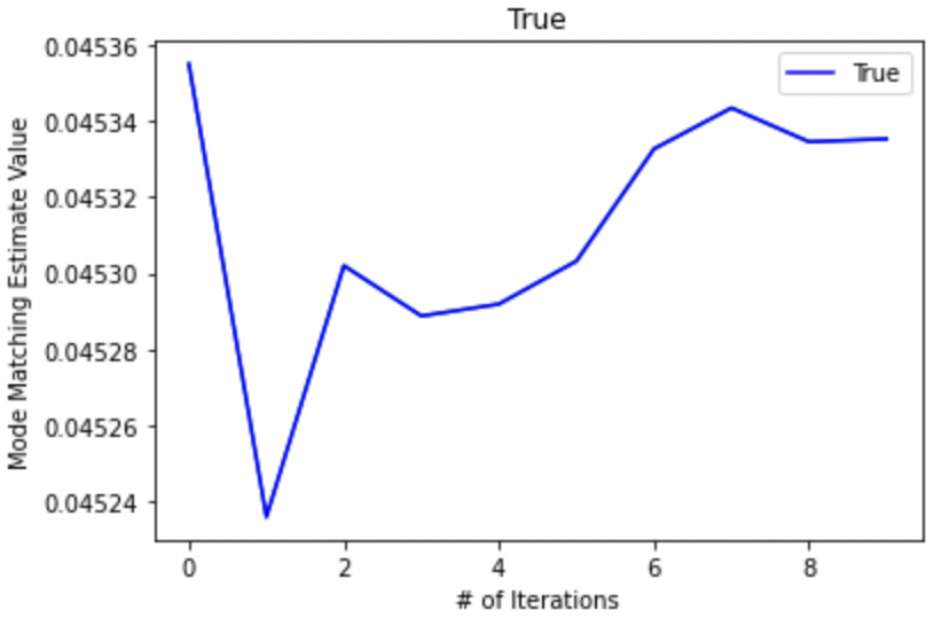

Figure 10: A Priori Estimate

The second plot provides the a priori estimate. It can be observed that the level of precision is very low. When testing the effectiveness of the Kalman filter a real physical system where the true state is unknown one can compare the precision. Comparing this second figure to the third figure, we can see that we would select this second figure in favor of the level of precision relative to the true state.

The posterior estimate gives the best representation of the true state. The level of precision is much higher than that of the a priori estimate. This confirms that the Kalman filter is a

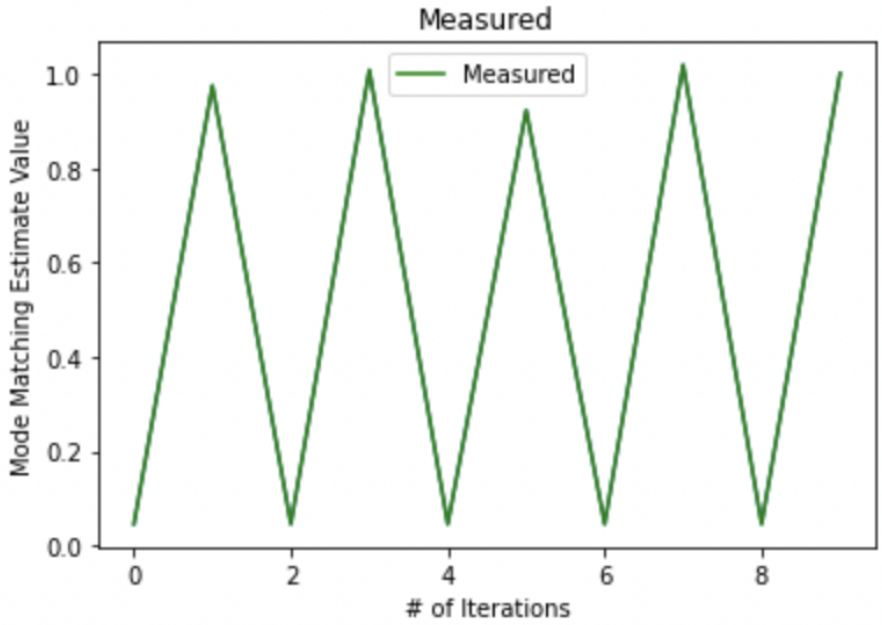

Figure 11: Simulated Measurement Data

viable candidate for estimating the state of the interferometer.

7 Conclusion

The Kalman filter's ability to process a posterior estimate of the system has refined the knowledge of the system. Preliminary execution has shown the filter is capable of taking radii of curvature, length of the arm cavity, width of the incoming beam, and mode of the cavity. After the successful implementation and testing of the software on this simple system, the next step should be put to the test with real data from LIGO detectors, so that real time estimates can be made of the state of the interferometer. The program will then be tweaked to its final version until the eigenmode matching is favorable.

References

[1] Aidan F. Brooks et al., *Overview of Advanced LIGO adaptive optics*. Applied Optics Vol. 55, No. 29 (2016).

[2] Aidan F. Brooks, *AWC Online Kalman Filter formalism and synthetic example*. Internal working note of the LIGO project

[3] Charlotte Bond et al., *Interferometer Techniques for Gravitational-Wave Detection*. arXiv:0909.3661v3 (2015).

[4] https://www.kalmanfilter.net/default.aspx

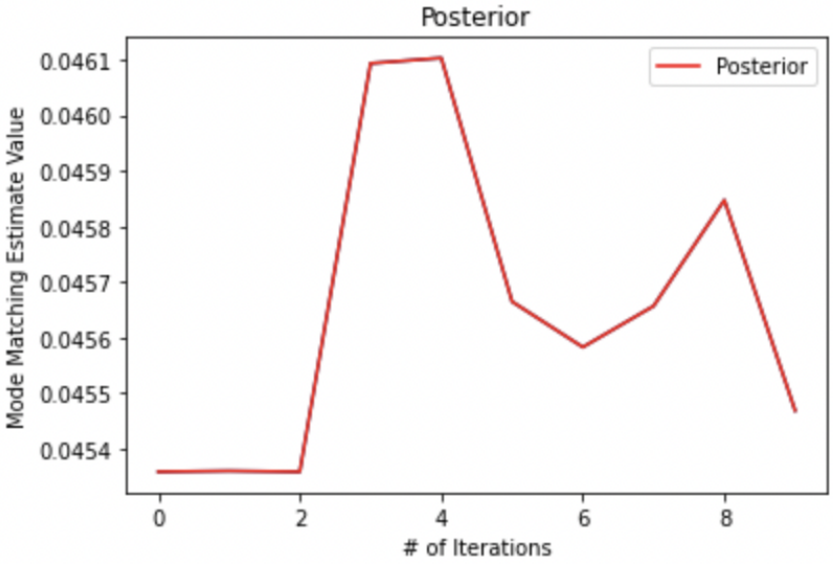

Figure 12: Posterior Estimate Generated by the Kalman Filter